PNNL-14617

Pacific Northwest
National Laboratory
Operated by Battelle for the
U.S. Department of Energy

Evaluation of Xenon Gas Detection as a Means for Identifying Buried Transuranic Waste at the Radioactive Waste Management Complex, Idaho National Environmental and Engineering Laboratory

P. E. Dresel
S. R. Waichler

April 2004

Prepared for the U.S. Department of Energy
under Contract DE-AC06-76RL01830

DISCLAIMER

PACIFIC NORTHWEST NATIONAL LABORATORY
operated by
BATTELLE
for the
UNITED STATES DEPARTMENT OF ENERGY
under Contract DE-AC06-76RL01830

Printed in the United States of America

Available to DOE and DOE contractors from the
Office of Scientific and Technical Information,
P.O. Box 62, Oak Ridge, TN 37831-0062;
ph: (865) 576-8401
fax: (865) 576-5728
email: reports@adonis.osti.gov

Available to the public from the National Technical Information Service,
U.S. Department of Commerce, 5285 Port Royal Rd., Springfield, VA 22161
ph: (800) 553-6847
fax: (703) 605-6900
email: orders@ntis.fedworld.gov
online ordering: http://www.ntis.gov/ordering.htm


This document was printed on recycled paper.

PNNL-14617

Evaluation of Xenon Gas Detection as a Means for Identifying Buried Transuranic Waste at the Radioactive Waste Management Complex, Idaho National Environmental and Engineering Laboratory

P. E. Dresel
S. R. Waichler

April 2004

Prepared for
the U.S. Department of Energy
under Contract DE-AC06-76RL01830

Pacific Northwest National Laboratory
Richland, Washington 99352

Summary

Xenon is produced as a fission product in nuclear reactors and through spontaneous fission of some transuranic (TRU) isotopes. Xenon, an inert rare gas, will be released from buried TRU waste. This document describes and evaluates the potential for analyzing xenon isotopes in soil gas to detect TRU waste in the subsurface at the Idaho National Environmental and Engineering Laboratory's Radioactive Waste Management Complex.

Two complementary methods for xenon isotope measurements are evaluated, radiometric analysis of short-lived radioxenon isotopes, and mass spectrometry for detection of stable xenon isotopes. The radioxenon analysis has the greatest sensitivity due to the lower background concentrations than the stable isotopes. Stable isotope ratios however may be used to distinguish irradiated fuel sources from pure spontaneous fission sources. The production rate and steady-state concentrations of the radioxenon isotopes are calculated.

Numerical modeling indicates that, under generalized burial ground conditions, the radioxenon isotopes will diffuse away from the waste and be found in the cap and adjacent to the burial ground at levels many orders of magnitude above the instrumental detection limit.

The greatest unknown in the evaluation is the release rate of xenon from the waste forms. This will be dependant on the type of waste and container integrity. The radioxenon isotopes will be most affected by slow release rates due to their short half lives.

Contents

Figures

Tables

1.0 Introduction

This paper describes a new technique for detection of transuranic (TRU) waste in the subsurface and evaluates the applicability of the technique to the Subsurface Disposal Area (SDA) at the Radioactive Waste Management Complex (RWMC) at the Idaho National Engineering and Environmental Laboratory (INEEL).

The technique is based on collecting soil gas samples from the vicinity of the waste and analyzing the xenon isotopes in the gas. The xenon isotopic composition is altered from atmospheric by spontaneous fission of TRU isotopes or by the presence of non-separated fission material (e.g., irradiated fuel). Xenon will diffuse readily from the source because it is a nearly inert gas. The method is analogous to the well-established methods of soil gas sampling for volatile organic compounds.

Two separate analytical methods are considered for application at the RWMC, radiometric counting of short-lived xenon isotopes and rare-gas mass spectrometry for stable xenon isotopes. The methods require different sample sizes and provide complementary information, as described below. The short-lived isotopes are indicative of active spontaneous fission in the waste, usually from plutonium-240. Because of the short half-lives, the ambient background for these isotopes is extremely low. Stable xenon isotopes are also produced by spontaneous fission but ambient backgrounds are higher due to the stable xenon isotopes of air. Stable xenon isotope signatures from reactor fission will persist as the gas diffuses slowly out of the fuel matrix.

The production of xenon isotopes will depend on the nature of the waste material. This report focuses predominantly on xenon isotope progenies from plutonium-240 because of its relatively high spontaneous fission rate and concentration of several percent in weapons grade plutonium. Other TRU isotopes such as americium-241 have low spontaneous fission rates and will not contribute significantly to the xenon signal.

In this paper the pertinent aspects of the RWMC site and wastes are first described. The theory behind the measurements is discussed and a literature review of related work is documented. Calculations related to the production rate and transport of the gas from the source are performed to evaluate the likelihood of successful detection.

2.0 Site Summary

This section provides only a brief description of the RWMC and the area of interest for applying soil gas sampling for the detection of TRU. Most of this information is from Holdren et al. (2002).

The RWMC is located in the southwestern quadrant of INEEL and encompasses 72 ha (177 acres). The SDA, which is the radioactive waste landfill at the RWMC, is the focus of this evaluation. The original landfill at the SDA was established in 1952 and expanded in 1958. The timeline for use of different disposal facilities in SDA is shown in Holdren et al. (2002), Figure 3.3. The waste disposal locations are shown in Figure 2.1.

Early disposal records, through around 1959, are sketchy. Miscellaneous radioactive waste was received from the precursor to INEEL, the National Reactor Testing Station (NRTS) and TRU-contaminated waste from the Rocky Flats Plant (RFP). The TRU-contaminated waste was interspersed with the NRTS waste. The RFP TRU-contaminated waste, packaged in drums or wooden crates, was stacked horizontally in pits and trenches. Trenches were excavated to basalt.

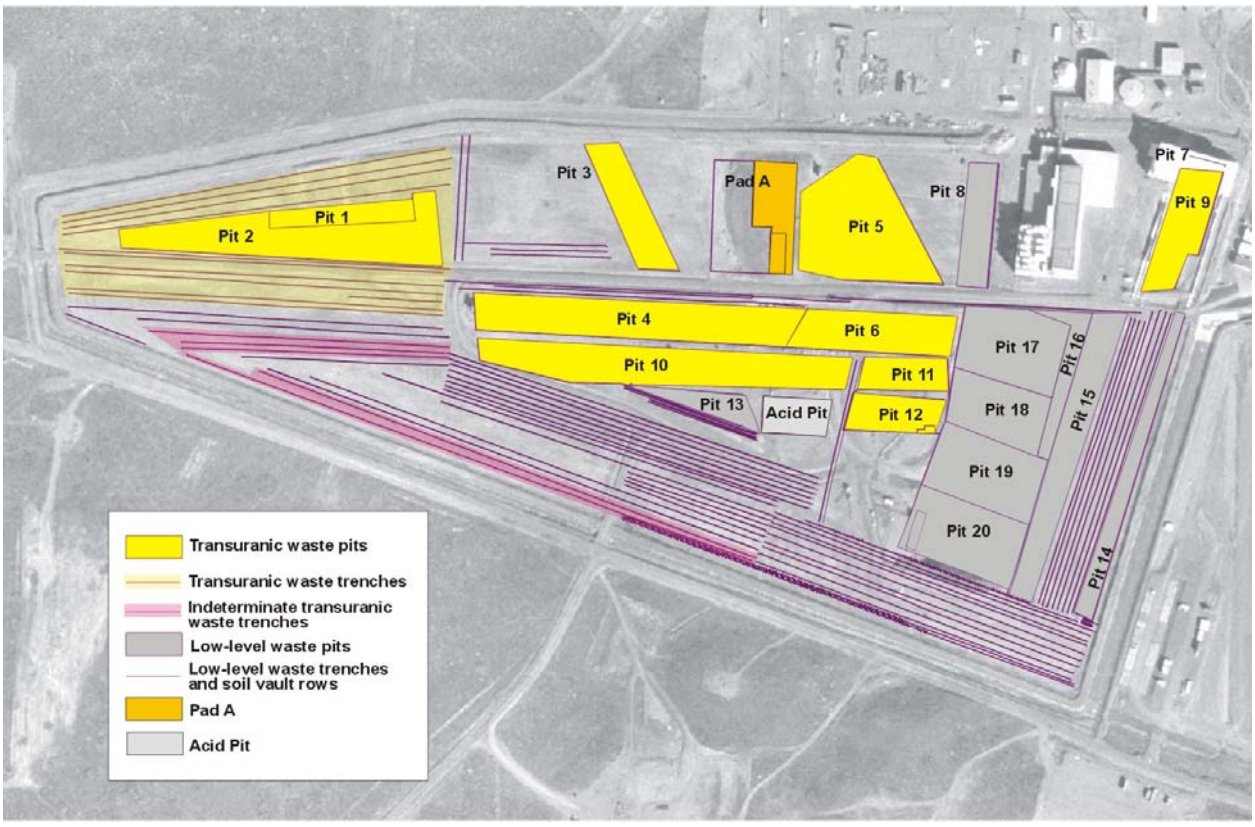

Figure 2.1. Transuranic and Low-Level Waste Disposal Locations in the Subsurface Disposal Area (from Holdren et al. 2002)

In addition to the NTRS and RFP waste, waste from off-site commercial generators was received beginning in 1960. Acceptance of off-site commercial waste ended in 1963.

Disposal practices were modified somewhat during 1964 to 1969. During this time period trenches were deepened and the trench bottoms were lined with at least 0.6 meter of soil. Beginning in November 1963 (and continuing until 1969), drums from RFP were dumped into pits rather than stacked to reduce labor costs and personnel exposures. Trenches were covered with a minimum of 0.9 meter of soil.

TRU waste was segregated into retrievable storage beginning in 1970. Since that time only low-level waste contaminated with less than 10 nCi/g TRU isotopes and mixed waste was disposed in SDA. During 1972 through 1978 Pad A was used for storage of low-level waste. This waste was stacked and covered with soil. During this time period the practice of compacting waste prior to disposal was begun. The use of trenches was discontinued in 1982, and no off-site waste has been received for disposal since the early 1990s. Beginning in 1985 a geotextile liner was incorporated into the underburden of pits.

From the site history, Trenches 1 through 10, Pits 1 through 12, and Pad A are of the greatest interest for detecting TRU waste in the subsurface. Plutonium inventory estimates for these locations are shown in Table 2.1. Pit 3 has the highest estimated plutonium concentration while Pit 12 has the lowest estimated concentration for the pits and Trench 2 has the lowest estimated concentration for the trenches. The relatively low inventories in Trenches 11 and 12 result from removal of all drums from these trenches during the Initial Drum Retrieval Project (McKinley and McKinney 1978). Approximately 1.83E+05 Ci of americium-241 were also disposed to the SDA. However, fission production of xenon from americium-241 is understood to be negligible, so it is not considered here. Similarly, neptunium-237, another contaminant of potential concern has a low spontaneous fission rate and will not be readily detectable through this technique.

Table 2.1. Plutonium Inventory Estimates for Disposal Locations within the Subsurface Disposal Area[(a)]

Disposal Location	Total Curies		Waste Volume m^3	Curies/m^3	
	Pu-239	Pu-240		Pu-239	Pu-240
Pit 1	6.15E+03	1.37E+03	12596	0.488273	0.108505
Pit 2	1.58E+04	3.51E+03	14869	1.062531	0.236118
Pit 3	3.32E+03	7.38E+02	2187	1.518614	0.33747
Pit 4	1.17E+04	2.61E+03	23500	0.497363	0.11122
Pit 5	5.48E+03	1.23E+03	8620	0.635513	0.142318
Pit 6	3.96E+03	8.86E+02	11857	0.333762	0.07476
Pit 9	3.32E+03	7.44E+02	5052	0.657408	0.14727
Pit 10	1.14E+04	2.55E+03	26675	0.426304	0.095495
Pit 11	1.35E+02	3.01E+01	505	0.266455	0.059666
Pit 12	1.50E+02	3.36E+01	829	0.181136	0.040514
Pad A	9.31E+02	2.08E+02	3880	0.239928	0.053536
Trench 1	3.64E+01	8.09E+00		unknown	unknown
Trench 2	3.41E+01	7.57E+00	1319	0.025839	0.005742
Trench 3	4.98E+01	1.11E+01	1004	0.04964	0.011031
Trench 4	8.80E+01	1.96E+01	1567	0.056136	0.012475
Trench 5	6.91E+01	1.54E+01	871	0.079337	0.01763
Trench 6	8.46E+01	1.88E+01	1121	0.075468	0.016771
Trench 7	7.20E+01	1.60E+01	663	0.108561	0.024125
Trench 8	1.19E+02	2.65E+01	873	0.136741	0.030387
Trench 9	1.00E+02	2.23E+01	436	0.229802	0.051067
Trench 10	5.49E+01	1.22E+01	329	0.166967	0.037104

(a) Inventory estimates from INEEL Geographic Information System laboratory mapping database filename: "rfp_zr_tru_el_v3.mxd" dated December 15, 2003. Waste volumes are for volumes of TRU, excluding overburden and underburden.

3.0 Theory

3.1 Isotopic Properties of Xenon

The atomic mass of the ten stable xenon isotopes ranges from 124 to 136. Six radioactive isotopes with half lives greater than 1 hour also exist: xenon-122, xenon-123, xenon-125, xenon-127, xenon-133, and xenon-135. Table 3.1 shows the natural abundance of the stable isotopes and the half-lives of the radioactive isotopes as presented in Parrington et al. 1996. Decay from meta-stable states is neglected for the purposes of this discussion, although it is of interest in monitoring of nuclear tests as discussed in Section 4.2.

Xenon is a high-yield fission product in nuclear reactors. The cumulative thermal neutron fission-yield for xenon isotopes from uranium-235 and plutonium-239 fission is also given in Table 3.1. Stable isotopes of tellurium and iodine block fission production of xenon isotopes 124 through 128 and 130. Xenon-129 production is also essentially blocked by iodine-129, which has a half-life of 1.57E7 years. For the purposes of this discussion, the direct fission yield of blocked isotopes is negligible.

Thermal neutron fission in reactors will be a mixture of uranium-235 fission and plutonium-239 fission, with the plutonium-239 contribution increasing with higher burn-up in the reactor. Although the fission yield curves are different for uranium-235 and plutonium-239, the differences are not large in the xenon isotopes of interest (Figure 3.1).

Table 3.1. Natural Abundance, Half-Life, and Thermal Neutron Fission Yield of Xenon Isotopes with Mass between 124 and 136

Isotope	Natural Abundance (atom %)	Half Life (from ground state)	U-235 Fission Yield (%)	Pu-239 Fission Yield (%)
Xe-124	0.10		blocked	blocked
Xe-125		17.1 hr	blocked	blocked
Xe-126	0.09		blocked	blocked
Xe-127		36.4 d	blocked	blocked
Xe-128	1.91		blocked	blocked
Xe-129	26.4		blocked[(a)]	blocked[(a)]
Xe-130	4.1		blocked	blocked
Xe-131	22.2		2.89	3.86
Xe-132	26.9		4.31	5.41
Xe-133		5.243 d	6.70	7.02
Xe-134	10.4		7.87	7.68
Xe-135		9.10 hr	6.54	7.6
Xe-136	8.9		6.32	7.1
(a) Fission production of Xe-129 is effectively blocked by long-lived I-129.				

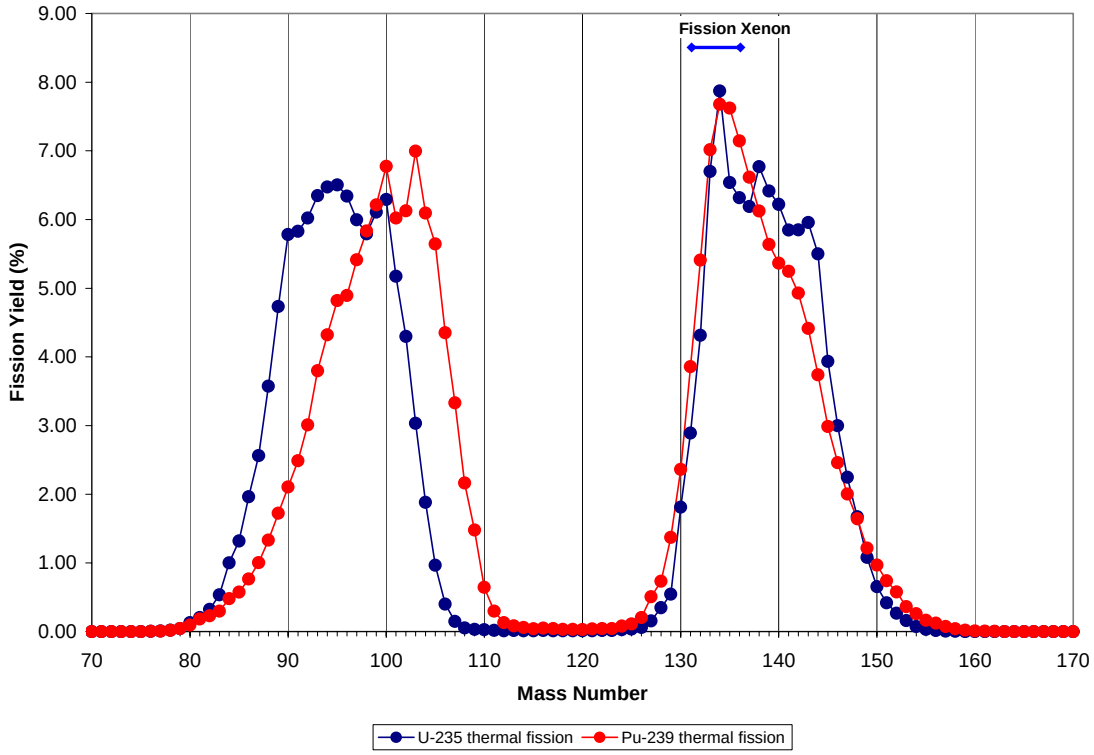

Figure 3.1. Thermal Neutron Fission Yield for U-235 and Pu-239

Disposal of unseparated irradiated fuel could provide a source for altered stable xenon isotopes, but the radioxenon isotopes from the reactor exposure would quickly decay away, except for continued production from spontaneous fission. At Hanford, stable xenon isotopes with ratios indicating reactor production were detected near the 618-11 burial ground; radioxenon isotopes were detected at the 216-Z-1A tile field (Dresel et al. 2003).

3.2 Xenon from Spontaneous Fission

Spontaneous fission of actinides produces xenon isotopes. Even mass-number isotopes of plutonium, americium, curium, and californium dominate spontaneous fission. Of these, plutonium-240 is produced to the greatest extent in plutonium production and power reactors. Weapons-grade plutonium contains less than 7 weight % plutonium-240. The plutonium content of fuel-grade plutonium is defined as 7 to 19 weight % plutonium-240. The plutonium-240 content of power reactor-grade plutonium is defined as greater than 19 weight % (DOE 1996). In practice, the plutonium-240 content of weapons grade plutonium is ~6 atom %. (Note: atom % of plutonium-240 in irradiated reactor fuel is slightly lower than weight %. For the rest of this discussion, percentages will refer to atom % unless specified otherwise).

The rest of this discussion will focus on plutonium-240 as the most likely source of fission production in the subsurface. Spontaneous fission of plutonium-240 dominates the fission rate even in weapons-grade plutonium. A recent critical review of spontaneous fission half-lives gives a plutonium-240

spontaneous fission half-life of 1.14E11 years (Holden and Hoffman 2000). This leads to a spontaneous fission rate of 483 fissions $g^{-1}s^{-1}$. For comparison, the radioactive half-life for plutonium-240 alpha decay is 6,563 years and the spontaneous fission branching ratio is given as 5.75E-06 (Ekström and Firestone 1999) giving the same fission rate. The value published by Klett (1999), 920 n $g^{-1}s^{-1}$, leads to a somewhat lower fission rate of 418 fissions $g^{-1}s^{-1}$. The Holden and Hoffman (2000) fission rate will be used for calculations in this report.

The fission yield for xenon isotopes from spontaneous fission of plutonium-240 is not readily obtained from literature tabulations. Plutonium-240 spontaneous fission yields are not included in the ENDF/B-VI data review (England and Rider 1994). It is a reasonable assumption that the spontaneous fission yield curve for plutonium-240 will be similar to the thermal neutron fission yield for plutonium-239. In this case, spontaneous fission of plutonium-240 is analogous to neutron capture by plutonium-239 followed by a fission event. Schillebeeckx et al. (1992) indicate that the mass distribution for plutonium-240 spontaneous fission is somewhat narrower than that of plutonium-239 thermal neutron fission but they do not provide the fission yield data for plutonium-240 post-neutron spontaneous fission.

4.0 Relevant Xenon Isotope Studies

The only use of xenon isotopic measurements for detection of subsurface TRU contamination that we found in reviewing the literature was our proof-of-principle work presented to the Geological Society of America (Dresel et al. 2003). A similar method, using helium isotopic measurements in soil gas to detect subsurface tritium contamination has been used successfully at the Hanford Site (Olsen et al. 2000, 2001).

Two related applications of radioxenon measurements are detection of fuel element failure during reactor operations and in comprehensive test ban treaty verification. The treaty verification work is particularly relevant because the instrumentation used in our radioxenon analysis was developed for that purpose.

Previous applications of stable xenon isotopic studies in the environment have focused on cosmochemistry and geochemistry. These are mainly relevant because they provide a well understood baseline of xenon isotopes in the environment and because they produced the experience in isotopic analysis needed for our application. Fission-xenon has been identified in minerals from Achaean natural nuclear reactors in Africa. Other areas of interest for xenon isotopes include magnetic resonance imaging and medical anesthesiology/imaging.

4.1 Proof-of-Principle Soil Gas Study

Soil gas samples were collected from waste sites at the Hanford Site to measure xenon isotopes during fiscal year 2003. Gas for radioxenon analysis was collected from two locations within the 216-Z-1A tile field in the 200-West Area. The tile field received liquid waste containing ~57 kilograms of weapons grade plutonium. The samples were composited for analysis. The combined sample contained 16,400 mBq/standard cubic meter air of xenon-133 and 1,811 mBq/standard cubic meter air of xenon-135 (Figure 4.1). The instrument detection limit was 0.58 mBq/standard cubic meter air for xenon-133 and 3 mBq/standard cubic meter air for xenon-135.

Samples from the two locations at the 216-Z-1A tile field were also analyzed for stable xenon isotopes. One of the samples contained stable isotopes that were shifted from atmospheric ratios. In addition, three samples from the 618-11 burial ground were analyzed for stable xenon isotopes. The 618-11 burial ground received a wide variety of contact and remote handled research waste. The samples were collected from existing small diameter soil gas monitoring points outside the burial ground fence-line, which precluded collecting large volume samples for radioxenon analysis. The samples showed stable xenon isotope ratios altered from atmospheric abundances. Of note, the xenon-136 was elevated above the fission yield with respect to xenon-134 (Figure 4.2). This is explained by xenon-136 production by neutron capture on xenon-135 and, thus, indicates material that has been exposed to the high neutron flux in a nuclear reactor. The xenon-136 to xenon-134 is consistent with values predicted from modeling of fission products in Hanford reactors.

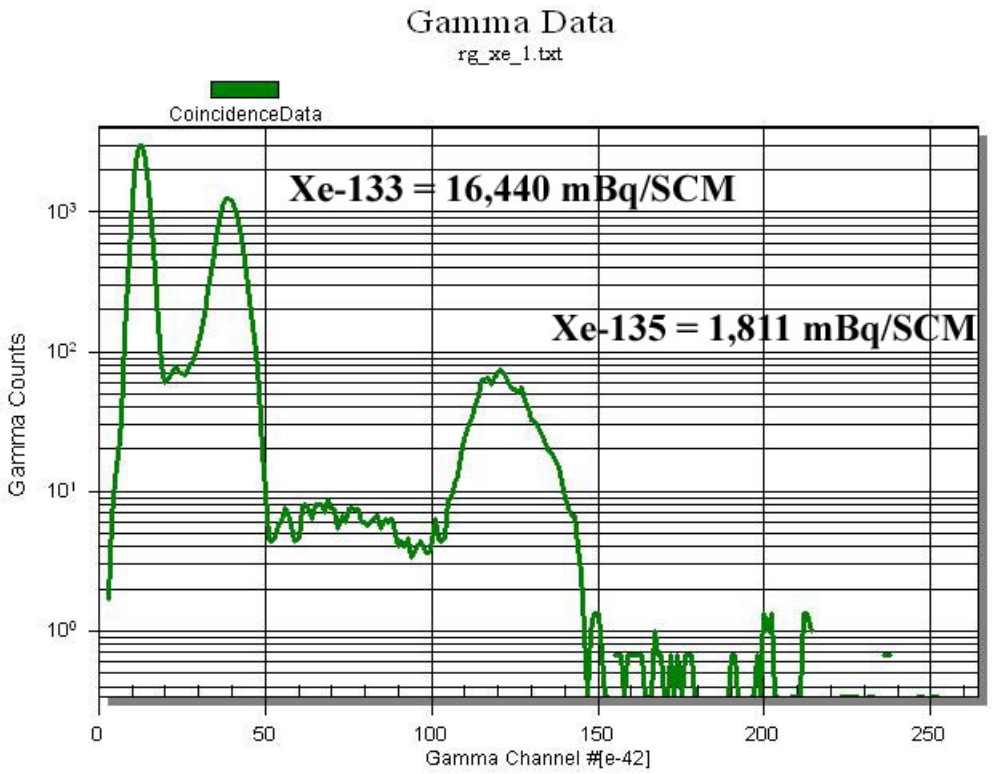

Figure 4.1. Beta-Gated Gamma Analysis of Soil Gas from the 216-Z-1A Tile Field, Hanford Site

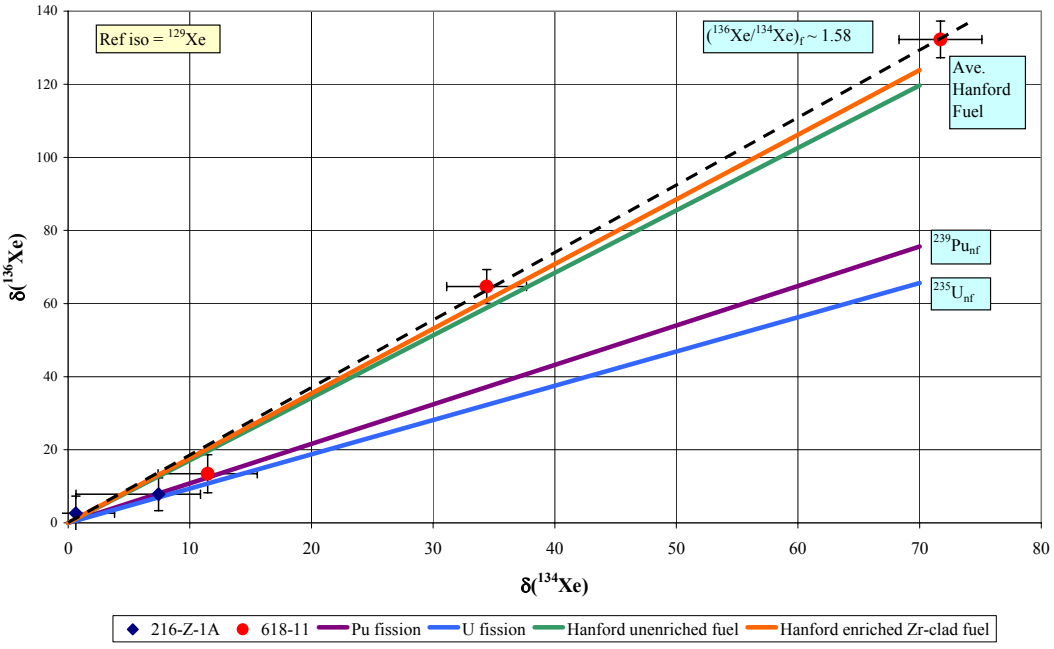

Figure 4.2. δ-xenon-136 vs. δ-xenon-134 for Soil Gas Samples from the Hanford Site. The reference isotope is xenon-129

4.2 Xenon Isotopic Studies in Reactor Operations and Fuel Reprocessing

Analysis of xenon and other noble gases can provide valuable information on nuclear reactor operations and on reprocessing activities. These studies show the potential for relating noble gas isotopes to the nuclear fuel cycle. Hudson (1993) discusses the application to monitoring of fuel reprocessing activities. Palcsu et al. (2001) discuss the measurement of krypton and xenon isotopes in cooling water as indicators of fuel element leakage. The relevance of these studies is that stable and radioactive xenon isotopes can be used to distinguish the anthropogenic contribution to gases in the environment.

4.3 Comprehensive Test Ban Treaty Verification

The investigation of xenon isotopes for comprehensive test ban treaty (CTBT) verification is relevant to the subsurface investigation because goals and techniques have similarities. The instrumentation used to detect subsurface TRU waste includes a modification of the Automated Radioxenon Sampling and Analysis (ARSA) system.

Since 1963, nuclear tests worldwide have taken place underground to limit the release of fission products. In 1996 the United Nations adopted the CTBT, and it was signed by 71 states including the United States of America and four other nuclear states. Article IV of the treaty outlines the verification regime including a global network of monitoring stations (www.ctbto.org). An overview of the radionuclide monitoring system is presented in Medici (2001). Radioxenon monitoring stations developed for the CTBT verification include the ARSA, developed at Pacific Northwest National Laboratory (Bowyer et al. 1996, 2002), and the SPALAX^{TM} developed by the French Atomic Energy Commission (Fontaine et al. 2004). These systems were designed for unattended sampling and analysis of ambient air in remote locations (however with connection to electrical power available). The ARSA system is shown in Figure 4.3.

Figure 4.3. Automated Radioxenon Sampling and Analysis System

Xenon isotopes are produced in large quantities during nuclear explosions and are difficult to contain; therefore, detection of fission xenon isotopes can be used to ascertain whether a detonation has occurred (Bowyer et al. 2002). The isotopes of interest for CTBT verification are metastable xenon-131, xenon-133, metastable xenon-133, and xenon-135. The isotope ratios will be close to the independent fission yield for rapid venting after an event and close to the cumulative fission yield for slower venting.

Testing of the ARSA and SPALAX systems has demonstrated that atmospheric background of radioxenon isotopes is extremely low and depends on the proximity to operating nuclear reactors and, in the case of xenon-133, medical facilities (McIntyre et al. 2001; Fontaine et al. 2004). Prototype ARSA units deployed at the Environmental Measurements Laboratory in New York State and Freiburg, Germany, detected three of the four radioxenon isotopes of interest. Metastable xenon-133 was not expected and was less than 0.2 mBq/standard cubic meter of air. The highest concentrations detected in the ARSA tests were for xenon-133, which were normally 0.7-1.5 mBq/standard cubic meter of air but ranged up to nearly 120 mBq/standard cubic meter of air for brief periods.

4.4 Geochemistry and Cosmochemistry

Fission xenon has previously been identified in mineral phases. Meshik et al. (2000) describe the identification of fission xenon in rocks from the natural nuclear reactors in Okelobondo, central Africa, in agreement with the results of previous workers. In their study of samples from reactor zone 13, they identify neutron-induced fission xenon in the uranium minerals and chemically fractionated fission xenon in an aluminum phosphate phase. The chemically fractionated fission xenon results from the migration of precursors in the decay chains that have varying half-lives and chemical properties, thus separating the xenon isotopes ultimately produced. In spite of the fractionation the fission origin can be deduced.

Most geochemical and cosmochemical studies of xenon are only of peripheral interest to the detection of TRU waste in the subsurface. An overview of the evolution of the earth and atmosphere discusses the role of xenon isotopes, particularly xenon-129, in interpreting early earth history (Allègre and Schneier 1994). Karoda and Myers (2001) present an evaluation of the variation of the xenon isotopic composition of the solar system, based on over 40 years of research into the subject. Their results indicate that the xenon isotope variation is a function of mass fractionation, spallation, stellar-temperature neutron decay reactions, plus beta decay of iodine-129 and spontaneous fission of plutonium-244 in the early universe.

Although the xenon isotopic composition of the mantle is shifted from that of the atmosphere (Porcelli and Wasserberg 1995), the atmospheric composition can be considered homogeneous with the exception of anthropogenic contributions. Subsurface fluids such as hydrocarbon reservoirs can show noble gas components, including xenon, from mantle and deep crustal processes as well as atmospheric contributions (e.g., Kennedy et al. 2002).

5.0 Analytical Methods

5.1 Radioxenon Analysis

The short-lived radioxenon isotopes must be analyzed promptly (within approximately a few days to a week from production, depending on the isotope and the concentration at time of sample collection). The ARSA system uses a series of chillers and sorbants to separate and concentrate xenon from air (Bowyer et al. 1996). The separation increases sensitivity by removing the major air components to reduce the volume and also by removing radioactive radon that can interfere with the counting. The removal of radon is important because the atmospheric background of radon is about 10 mBq/m^3 and certainly greater in soil-gas. A schematic of the system is shown in Figure 5.1. The system is designed for a flow rate of ~7 m^3/hr.

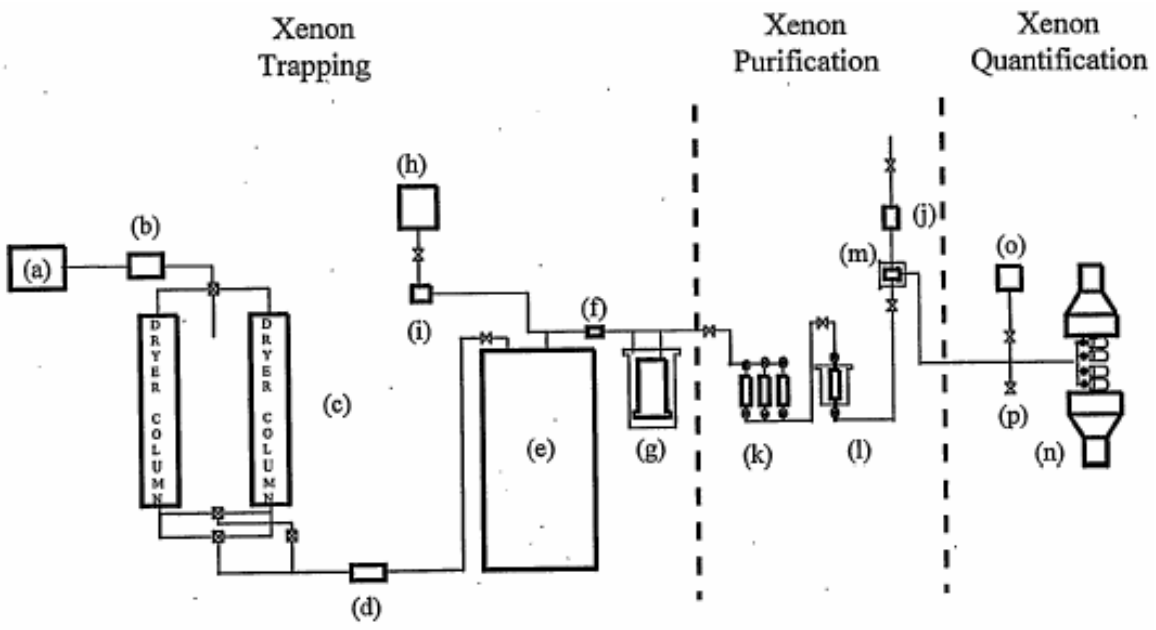

Figure 5.1. Schematic Illustration of Radioxenon Sampler/Analyzer. For simplicity the components needed for 100% duty cycle are not shown. The system consists of (a) a piston compressor pump (80 to 100 psig, 7 m^3/h), (b) heat exchanger, (c) dual air drying/CO_2 removal columns filled with 13X molecular sieve and Al_2O_3, (d) mass-flow controller for process air, (e) cryogenic air-chiller with output temperature -125 C, (f) initial radon "pre-trap", (g) cooled "main" charcoal trap for xenon trapping, (h) nitrogen bottle or generator, (i-j) mass flow controllers for nitrogen flow, (k) ascarite-based CO_2-removal traps, (l) cooled 5A-molecular sieve radon removal trap, (m) cooled, final small volume charcoal trap for xenon transfer into counting system, (n) NaI(Tl)-scintillating gas cell based beta-gamma coincidence spectrometer, (o) quadrupole residual gas analyzer, (p) path to archive bottles. From (Bowyer et al. 1996).

Xenon isotopes are quantified in a gas cell scintillation counter using beta-gamma coincidence counting. The beta signal is used as a gate for the photon detection system. Xenon-133 decays by emitting a 346 keV maximum energy beta particle in coincidence with an 81 keV gamma ray. However, the 81 keV gamma is internally converted so it will only be emitted in ~37% of the decay processes. In most of the other decay processes a beta particle, conversion electron, and 30 to 34 keV x-ray will be emitted in coincidence.

Xenon-135 decays by emitting an 910 maximum keV beta particle in coincidence with a 250 keV gamma (branching ratio 96%). Less than 10% of the 250 keV gamma rays undergo internal conversion.

The total xenon is analyzed with a quadrupole mass-spectrometer. The xenon is archived in a pre-evacuated sample bottle. The minimum detectable concentration is ~0.15 mBq/m^3 for xenon-133 and 0.3 mBq/m^3 for xenon-135 for an 8 hour collection (Bowyer et al. 2002).

5.2 Stable Xenon Analysis

Stable xenon isotopes are measured on an all metal high-resolution magnetic-sector noble gas mass spectrometer. The sample is purified by passing over a series of cold traps and metal alloy getters to remove CO_2, H_2O, N_2, etc. The residual noble gas fraction is adsorbed onto activated carbon at 27 K, and sequentially desorbed into the mass spectrometer by heating to different temperatures.

In addition to the xenon isotopic analysis, the samples are analyzed for selected isotopes of helium, neon, krypton, and argon in order to determine any shifts in rare gas ratios from atmospheric values.

5.3 Sampling Methods

Sampling for stable xenon isotopes is fairly straightforward since only small volumes of gas are needed. Samples can be collected from standard soil gas sampling points. Best results would be attained for samples collected deep enough to be beneath the zone of barometric pumping of air into the subsurface. Sample points should also be deep enough so that surface air is not entrained into the sample during the sampling event. Since concentrations of fission isotopes will decrease away from the source, points close to the source area are most likely to see a shift in isotopic ratios from background air. Samples are collected into a 30-milliliter stainless-steel pressure vessel pressurized to ~15 pounds per square inch (psi) with a diaphragm pump. The sample collection method is the same as used for helium isotope sampling described in Olsen et al. (2000 and 2001) (Figure 5.2).

The extremely low background of radioxenon isotopes and the ability to separate xenon from air mean that it is practical to process large volumes of soil gas in order to achieve excellent sensitivity. However, methods then are needed to collect large volumes of soil gas. The samples must also be analyzed rapidly to minimize the decay of the radioxenon isotopes after collection.

Samples to date have been collected into evacuated full size gas cylinders pressurized to ~2,000 psi with a compressor designed for filling scuba tanks (Figure 5.3). Samples were collected through ~1.27-centimeters interior-diameter steel tubing and a pre-filter to remove particulate material

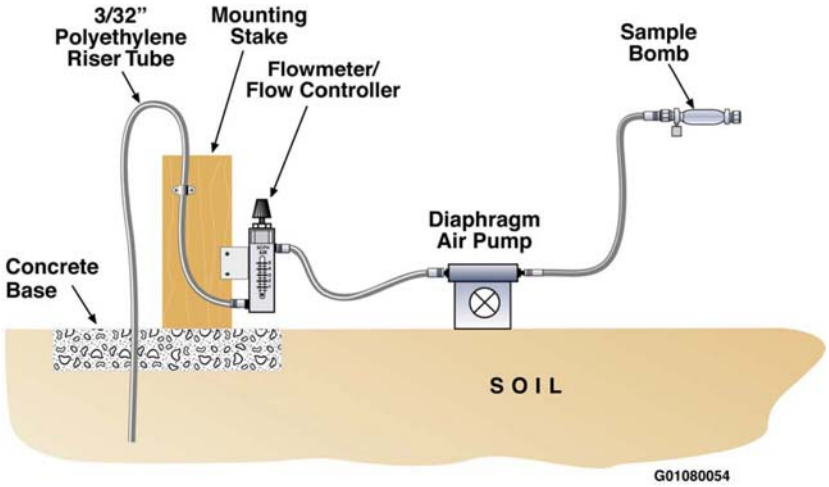

Figure 5.2. Schematic Diagram of Soil-Gas Sampling System Used for Collection of Stable Isotope Samples

Figure 5.3. Pump and Sample Cylinders for Radioxenon Collection

(Figure 5.4). The gas tanks were transported to the laboratory where the gas was metered into the ARSA system, followed by make-up air to match the volume needed for a measurement cycle (8 hours).

Another option is to mount the ARSA system in a mobile laboratory and transport it to the work site. The samples then can be pumped directly into the system. This would avoid delay between sampling and analysis and allow for the processing of even larger sample volumes with less or no make-up gas. Some upgrades are needed to deploy the system in this manner.

Figure 5.4. Sampling Point for Radioxenon Collection

6.0 Xenon Production

Spontaneous fission provides an ongoing source of xenon in TRU waste. As discussed in the preceding sections, spontaneous fission of plutonium-240 will be a major contributor in most plutonium bearing waste. This section presents calculations of the radioxenon production rate from plutonium-240 spontaneous fission. Calculations are then presented to indicate the levels of xenon isotopes that would be present at equilibrium with plutonium-240 in the waste. These levels are compared to detection limits to indicate whether their presence may be detectable by analysis of soil-gas radioxenon isotopes.

6.1 Production Rate

The xenon production rate is a function of the spontaneous fission rate and the fission yield of the isotopes. The equations are developed for xenon-133 and are similar for xenon-135.

From the plutonium-240 spontaneous fission half-life, 1.14E11 years or 3.60E18 seconds (see Section 3.2), the decay constant, $\lambda^{\eta}_{Pu\text{-}240}$:

$$\lambda^{\eta}_{Pu\text{-}240} = \ln(2)/ T_{½} = 1.93E\text{-}19\ s^{-1} \quad (6.1)$$

Multiplying by the fission yield of xenon-133, 7.02%, gives the effective decay constant for production of xenon-133 from spontaneous fission, $\lambda^{Xe\text{-}133}_{Pu\text{-}240}$:

$$\lambda^{Xe\text{-}133}_{Pu\text{-}240} = \lambda^{\eta}_{Pu\text{-}240} * 0.0702 = 1.35E\text{-}20\ s^{-1} \quad (6.2)$$

The value for $\lambda^{Xe\text{-}133}_{Pu\text{-}240}$ is the production rate of xenon-133 atoms per atom plutonium-240 per second. This is equivalent to a production rate of 3.39E+01 atoms per gram of plutonium-240 per second.

Calculations for xenon-135 are similar.

$$\lambda^{Xe\text{-}135}_{Pu\text{-}240} = \lambda^{\eta}_{Pu\text{-}240} * 0.076 = 1.46E\text{-}20\ s^{-1} \quad (6.3)$$

The fission yield of xenon-135 is slightly higher than the fission yield of xenon-133, so the xenon-135 production rate in terms of atoms per gram plutonium-240 per second, 3.67E+01, is slightly higher than that of xenon-133. Table 6.1 shows the production rate for the average plutonium-240 concentrations estimated for each waste unit at the RWMC. Production rates are expressed in both atoms $m^{-3}\ s^{-1}$ and mBq $m^{-3}\ s^{-1}$. These rates are used for input to the gas transport model discussed in Section 7.

6.2 Secular Equilibrium

The radioxenon isotope concentrations will build up to steady-state, secular equilibrium values in the absence of transport because the half-lives are shorter than the fission half-life of plutonium-240. This provides a bounding value for the gas concentrations. For the purposes of the calculation it is assumed that secular equilibrium is attained between the plutonium-240 in a unit volume of soil and the xenon-133 or xenon-135 in the soil gas.

Table 6.1. Spontaneous Fission Xenon Production Rates for Waste Units at the RWMC Based on Estimated Pu-240 Inventories

Location	Pu-240		Xe-133 production		Xe-135 production	
	Ci/m^3	g/m^3	$at/(m^3*s)$	$mBq/(m^3*s)$	$at/(m^3*s)$	$mBq/(m^3*s)$
Pit 1	1.09E-01	4.78E-01	1.62E+01	2.48E-02	1.76E+01	3.72E-01
Pit 2	2.36E-01	1.04E+00	3.53E+01	5.40E-02	3.82E+01	8.09E-01
Pit 3	3.37E-01	1.49E+00	5.05E+01	7.72E-02	5.46E+01	1.16E+00
Pit 4	1.11E-01	4.90E-01	1.66E+01	2.55E-02	1.80E+01	3.81E-01
Pit 5	1.42E-01	6.27E-01	2.13E+01	3.26E-02	2.30E+01	4.88E-01
Pit 6	7.48E-02	3.29E-01	1.12E+01	1.71E-02	1.21E+01	2.56E-01
Pit 9	1.47E-01	6.49E-01	2.20E+01	3.37E-02	2.38E+01	5.05E-01
Pit 10	9.55E-02	4.21E-01	1.43E+01	2.19E-02	1.55E+01	3.27E-01
Pit 11	5.97E-02	2.63E-01	8.92E+00	1.37E-02	9.66E+00	2.04E-01
Pit 12	4.05E-02	1.79E-01	6.06E+00	9.27E-03	6.56E+00	1.39E-01
Pad A	5.35E-02	2.36E-01	8.01E+00	1.23E-02	8.67E+00	1.83E-01
Trench 1	unknown	unknown	unknown	unknown	unknown	unknown
Trench 2	5.74E-03	2.53E-02	8.59E-01	1.31E-03	9.30E-01	1.97E-02
Trench 3	1.10E-02	4.86E-02	1.65E+00	2.52E-03	1.79E+00	3.78E-02
Trench 4	1.25E-02	5.50E-02	1.87E+00	2.85E-03	2.02E+00	4.27E-02
Trench 5	1.76E-02	7.77E-02	2.64E+00	4.03E-03	2.85E+00	6.04E-02
Trench 6	1.68E-02	7.39E-02	2.51E+00	3.84E-03	2.72E+00	5.75E-02
Trench 7	2.41E-02	1.06E-01	3.61E+00	5.52E-03	3.91E+00	8.26E-02
Trench 8	3.04E-02	1.34E-01	4.54E+00	6.95E-03	4.92E+00	1.04E-01
Trench 9	5.11E-02	2.25E-01	7.64E+00	1.17E-02	8.27E+00	1.75E-01
Trench 10	3.71E-02	1.63E-01	5.55E+00	8.49E-03	6.01E+00	1.27E-01

For xenon-133 beta decay, $T_{½}$ = 5.24 days or 453,000 seconds:

$$\lambda^{\beta}_{Xe\text{-}133} = \ln(2)/ T_{½} = 1.531E\text{-}06\ s^{-1} \tag{6.4}$$

At secular equilibrium the decay rate of xenon-133 equals the production rate (i.e., the decay rate of plutonium-240 times the fission yield of xenon-133):

$$N_{Xe\text{-}133} * \lambda^{\beta}_{Xe\text{-}133} = N_{Pu\text{-}240} * \lambda^{Xe\text{-}133}_{Pu\text{-}240} \tag{6.5}$$

where N is the number of atoms of each isotope. Thus, the atoms X-133 present per atom Pu-240 is:

$$\lambda^{Xe\text{-}133}_{Pu\text{-}240}/ \lambda^{\beta}_{Xe\text{-}133} = 8.83E\text{-}15 \tag{6.6}$$

For xenon-135, $T_{½}$ = 9.10 hours or 33,000 seconds:

$$\lambda^{\beta}_{Xe\text{-}135} = \ln(2)/ T_{½} = 2.116E\text{-}05\ s^{-1} \tag{6.7}$$

$$\lambda^{Xe\text{-}135}_{Pu\text{-}240}/ \lambda^{\beta}_{Xe\text{-}135} = 6.92E\text{-}16 \tag{6.8}$$

Estimates of plutonium-240 concentrations for each disposal area were provided by INEEL site personnel (see Table 2.1). The concentrations given in Ci/m^3 soil are converted to atoms/m^3 soil (C_{Pu-240}), then the xenon-133 equilibrium soil gas concentration (C_{Xe-133}) is calculated from the secular equilibrium ratio, assuming all xenon for a given soil volume is in the soil gas:

$$C_{Xe-133} = C_{Pu-240} * n * \lambda^{Xe-133}{}_{Pu-240} / \lambda^{\beta}{}_{Xe-133} \quad (6.9)$$

Where n is the porosity (set to 0.5).

The activity-concentration can be calculated from the atom-concentration or from simply setting the xenon-133 activity equal to the plutonium-240 alpha activity times the spontaneous fission branching ratio times the xenon-133 fission yield. For convenience in comparing to instrument detection limits the results are converted to mBq/m^3 of soil gas.

Because the production rate is slightly higher for xenon-135, the steady state activity for xenon-135 will be slightly higher, too. The atom concentration of xenon-135 at steady state, however, will be much lower than that of xenon-133.

The results of the calculations for different waste units are given in Table 6.2. Secular equilibrium concentrations are far above the detection limits for the ARSA system. However, these values probably

Table 6.2. Secular Equilibrium Xenon Concentrations for Each Disposal Unit in the RWMC Based on Estimated Pu-240 Inventories

Location	Pu-240		Xe-133	Xe-135
	Ci/m^3	atom/m^3 air	mBq/m^3 air	mBq/m^3 air
Pit 1	0.1085051	2.40E+21	3.24E+04	3.51E+04
Pit 2	0.23611791	5.22E+21	7.06E+04	7.64E+04
Pit 3	0.33746977	7.46E+21	1.01E+05	1.09E+05
Pit 4	0.11122021	2.46E+21	3.33E+04	3.60E+04
Pit 5	0.14231781	3.15E+21	4.26E+04	4.61E+04
Pit 6	0.07476014	1.65E+21	2.24E+04	2.42E+04
Pit 9	0.14726975	3.25E+21	4.40E+04	4.77E+04
Pit 10	0.09549509	2.11E+21	2.86E+04	3.09E+04
Pit 11	0.05966588	1.32E+21	1.78E+04	1.93E+04
Pit 12	0.04051368	8.95E+20	1.21E+04	1.31E+04
Pad A	0.05353601	1.18E+21	1.60E+04	1.73E+04
Trench 1	unknown	unknown	unknown	unknown
Trench 2	0.0371038	8.20E+20	1.11E+04	1.20E+04
Trench 3	0.00574208	1.27E+20	1.72E+03	1.86E+03
Trench 4	0.0110311	2.44E+20	3.30E+03	3.57E+03
Trench 5	0.01247463	2.76E+20	3.73E+03	4.04E+03
Trench 6	0.01763038	3.90E+20	5.27E+03	5.71E+03
Trench 7	0.01677077	3.71E+20	5.02E+03	5.43E+03
Trench 8	0.02412476	5.33E+20	7.21E+03	7.81E+03
Trench 9	0.03038688	6.72E+20	9.09E+03	9.84E+03
Trench 10	0.05106703	1.13E+21	1.53E+04	1.65E+04

provide an upper bound limit on the concentrations that can be expected in the samples. Decay of xenon prior to transfer to the gas phase and decay/dispersion during transport to the sampling point may reduce the concentrations. The impacts of the release rate to the gas phase are difficult to quantify without further information. Transport effects in the gas phase are discussed in Section 7.

6.3 Calculation of Time Since Production From Relative Decay Rates of Xenon-133 and Xenon-135

The average time between xenon production and sampling can be calculated if the concentrations of both xenon-133 and xenon-135 are known, because of the different half-lives. For any radionuclide:

$$N = N_0 e^{-\lambda t} \tag{6.10}$$

Where N is the number of atoms remaining N_0 is the original number of atoms, and t is the time since the starting time. Thus, the atom ratio of xenon-135 to xenon-133 at time t is:

$$\frac{^{135}N}{^{133}N} = \frac{^{135}N_0 e^{-^{135}\lambda t}}{^{133}N_0 e^{-^{133}\lambda t}} \tag{6.11}$$

Solving for t gives:

$$t = \frac{\ln\left(\frac{^{135}N}{^{133}N} \bullet \frac{^{133}N_0}{^{135}N_0}\right)}{^{133}\lambda - ^{135}\lambda} \tag{6.12}$$

The ratio at time zero is the ratio of the fission yields. The average time is of interest for evaluating gas transport models and to provide some indication of release rates from the waste material.

7.0 Gas Phase Transport Calculations

It is critical that the xenon gas moves from the waste to the sampling points prior to decay in order to successfully detect the radioxenon isotopes. Transport calculations were performed in order to predict the radioxenon concentrations in and surrounding the waste units. The calculations indicate that transport through the vadose zone to sampling points is unlikely to be a significant limitation on the success of the technique for detecting xenon-133. The effect is somewhat greater for xenon-135 because of its shorter half-life.

7.1 Model Introduction

The Subsurface Transport Over Multiple Phases (STOMP) model (White and Oostrom 2000, 2004) was used to simulate the diffusion of xenon gas from a subsurface source. Steady-state concentrations attained after long time were reported. The spatial domain was represented with a two-dimensional vertical cross-section that represents the right half of a symmetric waste trench (Figure 7.1). Initial conditions for the gas modeling were derived by running STOMP with only water and air for fifty years. For simulating xenon gas, a constant release rate was used and STOMP was run for 200 days. Two isotopes of xenon gas were simulated, xenon-135 and xenon-133, with half-lives of 5.243 days and 9.10 hours, respectively. Release of xenon from the waste was specified with two concentration units: atoms/m3 and mBq/m3. For convenience, the two release units were incorporated as additional species in the STOMP simulations, for a total of four simulated gas species.

A base case and six additional cases to evaluate sensitivity or check assumptions were simulated. The additional cases used the base case input values except for the particular input being changed.

1. Base case. Xenon release based on Pit 3 (maximum concentration), natural recharge rate = 50 millimeter per year, residual saturation in sediments = 0.292, Millington and Quirk (1959) tortuosity, and constant atmospheric pressure.

2. Test of linear scaling. Xenon release based on Pit 12 (minimum concentration).

3. Infiltration rate = 10 millimeters per year

4. Residual moisture content in sediments = 0.10.

5. Small tortuosity (sediments = 3, basalt = 1)

6. Large tortuosity (sediments = 5, basalt = 2)

7. Atmospheric pumping. Sinusoidal change in atmospheric pressure with period = 20 days.

Model output was evaluated for spatial and temporal trends. Cross-sections of steady-state concentration are provided in Section 7.3, along with time-series and tabulated values of xenon concentration at the target location of interest, 75 centimeters below ground surface along the waste centerline (left boundary of the model domain). This target depth represents a soil gas monitoring point installed in the cover without penetrating the waste.

7.2 Model Parameterization

The model domain was 25 meters wide by 30 meters tall. Grid spacing was 0.25 meters in all dimensions, resulting in 12,000 nodes. STOMP was run in Water-Air mode, with mass transport for xenon. Initial water and air gradients were static. Molecular diffusion of xenon in the gas phase was the major process affecting its transport in all cases. Dissolution of xenon in vadose zone moisture and subsequent drainage were minor processes in all cases. In Case 7, atmospheric pumping introduced advection and dispersion as additional processes governing xenon transport. In the rest of this report, model input description refers to the base case unless otherwise noted.

7.2.1 Soil/Rock

Four subsurface soil/rock types were specified: waste, overburden, underburden, and basalt (Figure 7.1). The first three types were given the same physical properties as provided by INEEL for sediments. These units could be easily differentiated in the future if needed. All properties were taken from INEEL site characterization data where provided, or from the literature.

7.2.2 Xenon-Air and Xenon-Aqueous Interaction

The model input parameters for xenon-air and xenon-aqueous interactions are shown in Table 7.1. The parameters are taken from literature values as indicated or estimated, based on professional judgment. Model parameters for soil properties are listed in Table 7.2.

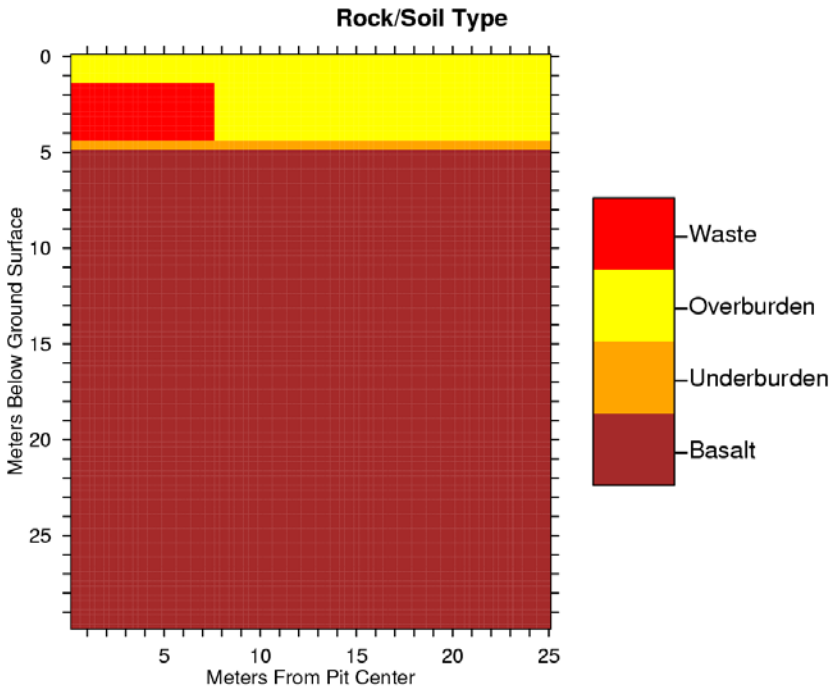

Figure 7.1. Spatial Domain for Model. This two-dimensional vertical cross-section domain represents the right half of a symmetric waste burial configuration.

Table 7.1. Model Parameters for Gas-Air and Gas-Aqueous Interactions

Parameter	Base Case Value	Comment
Aqueous phase molecular diffusion coefficient	0.10e-5 cm^2/s	Estimated as 5 orders of magnitude lower than gas phase diffusion
Gas phase molecular diffusion coefficient	0.10 cm^2/s	Computed using methods in Poling et al. (2001)
Gas-aqueous partition function	Constant	Other option is temperature-dependent
Gas-aqueous partition coefficient	9.09	mol Xe gas/m^3 gas / mol Xe aq./m^3 aq. (unitless) Current value is from paper by Pollack et al. (1989) at 25 C
Radioactive half-life	5.243 days	For Xe-133
	9.10 hours	For Xe-135
Solid-aqueous partition coeff.	0 m^3/kg	mol Xe sorbed/kg solid / mol Xe aq./m^3 aq.

Table 7.2. Model Parameters for Soil Properties. Base case values given here; alternative values for sensitivity analysis cases are given in the text.

Parameter	Overburden, Underburden, and Waste	Basalt	Source
Particle density	2700 kg/m^3	2700 kg/m^3	Magnuson and Sondrup (1998)
Porosity	0.5	0.05	Magnuson and Sondrup (1998)
Effective porosity	0.5	0.05	Magnuson and Sondrup (1998)
Specific storativity	1e-12 m^{-1}	1e-12 m^{-1}	Freeze and Cherry (1979)
Tortuosity function			Millington and Quirk (1959)
Horizontal hydraulic conductivity	0.565 m/day	7.48 m/day	Magnuson and Sondrup (1998)
Vertical hydraulic conductivity	0.565 m/day	0.831 m/day	Magnuson and Sondrup (1998)
Saturation function			van Genuchten (1980)
alpha	1.066 m^{-1}	10.0 m^{-1}	Magnuson and Sondrup (1998)
n	1.523	2.5	Magnuson and Sondrup (1998)
Minimum saturation	0.292	0.001	Magnuson and Sondrup (1998)

7.2.3 Initial and Boundary Conditions

STOMP was first run with water and air for 50 years to arrive at a steady-state condition with respect to soil moisture (Figure 7.2). The initial water and air gradients for this run were set to hydrostatic. The top model boundary (ground surface) was set to a constant atmospheric air pressure, water infiltration = 50 millimeters per year water, and zero xenon concentration. The left and right model boundaries were no-flux. The bottom model boundary was set to saturation for water (water table), and zero xenon concentration. Simulation of the seven main cases was done with STOMP's Restart mode, wherein the final state from the water/air-only simulation was used for the initial conditions to the gas simulation. The initial soil moisture state demonstrates a capillary barrier at the contact between sediments and basalt, and the resulting decrease in moisture content upward from the contact.

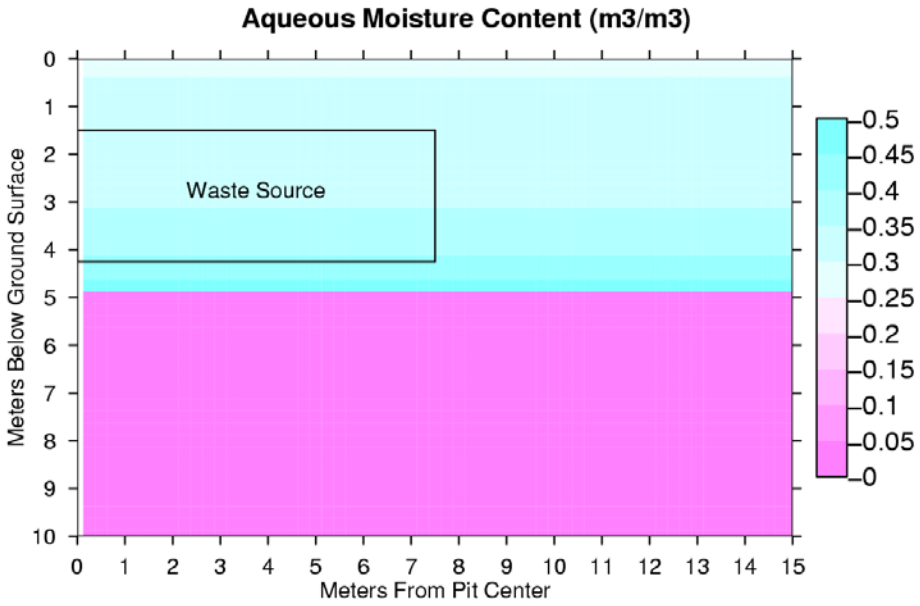

Figure 7.2. Steady-State Moisture, Base Case

For Case 7, a sinusoidal atmospheric pressure boundary condition developed by Magnuson and Sondrup (1998) was applied to the ground surface. The period was 20 days, and the amplitude was 1.4 kPa.

7.2.4 Xenon Source

Xenon was released uniformly over the waste portion of the model domain at the rates in Table 7.3.

7.3 Model Results

The modeled steady-state gas concentrations for xenon-133 and xenon-135 in proximity to the waste source are shown in Figure 7.3 and Figure 7.4. Concentrations for the two xenon isotopes are shown in a horizontal trajectory at a depth of 75 centimeters in Figures 7.5 and 7.6. Concentrations along the vertical trajectory at the left boundary (waste pit centerline) from the top of the waste source to ground surface are shown in Figures 7.7 and 7.8. Steady-state gas concentrations were attained relatively rapidly, as shown in the base case time-series plots of moisture content and gas concentrations (Figure 7.9). The time for xenon-133 (5-day) gas concentrations to reach a level within 0.1% of the final concentration ranged from 4 to 11 days. The base case required 4.7 days. The water-gas mass fraction ratio for xenon was 0.014,

Table 7.3. Xenon Source Release Rates

Location	Xe-133, half-life=5 days		Xe-135, half-life=9 hours	
	(atoms m^{-3} sec^{-1})	(mBq m^{-3} sec^{-1})	(atoms m^{-3} sec^{-1})	(mBq m^{-3} sec^{-1})
Pit 3 (Base case)	5.046596E+01	7.723478E-02	5.463551E+01	1.156069E+00
Pit 12 (Case 2)	6.058502E+00	9.272134E-03	6.559062E+00	1.387875E-01

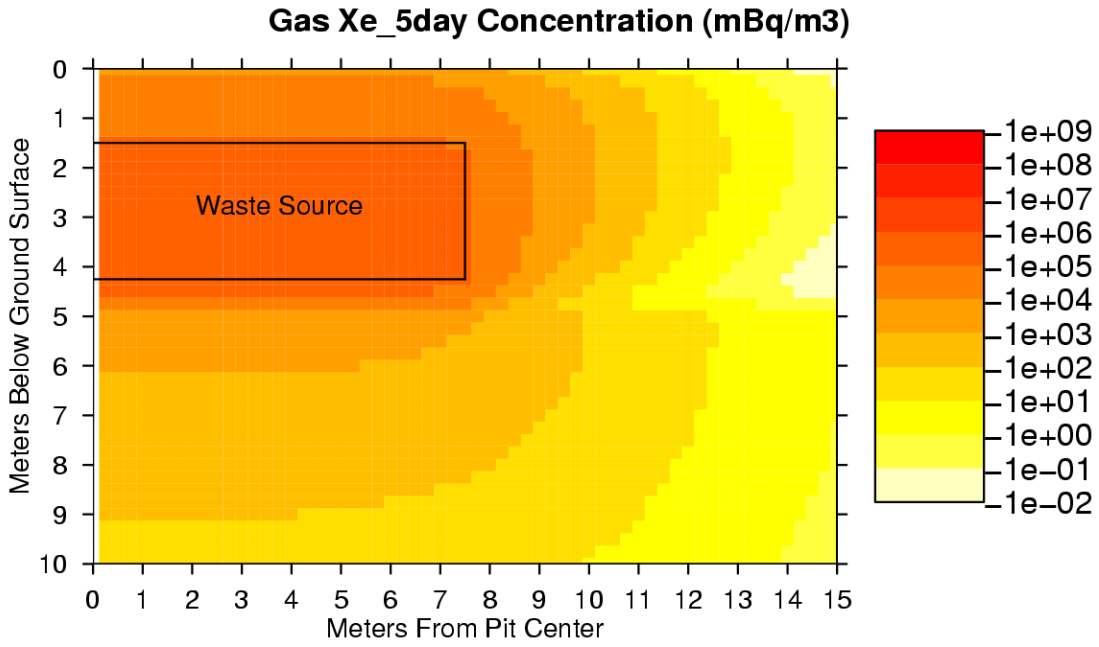

Figure 7.3. Base Case Steady-State Xe-133 Gas Concentration

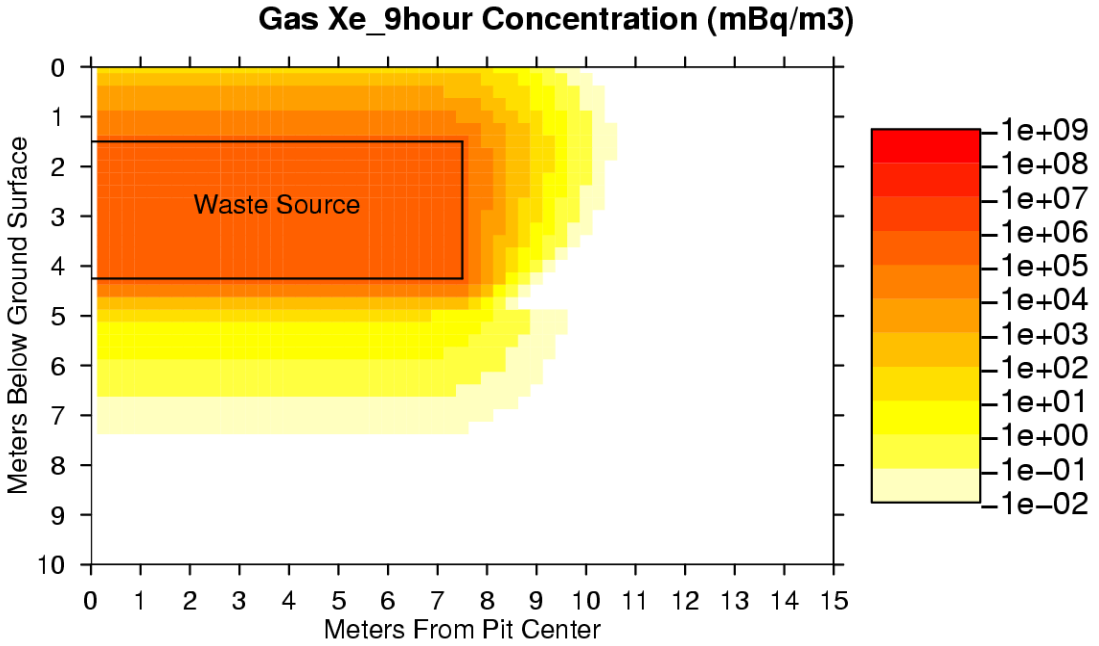

Figure 7.4. Base Case Steady-State Xe-135 Gas Concentration

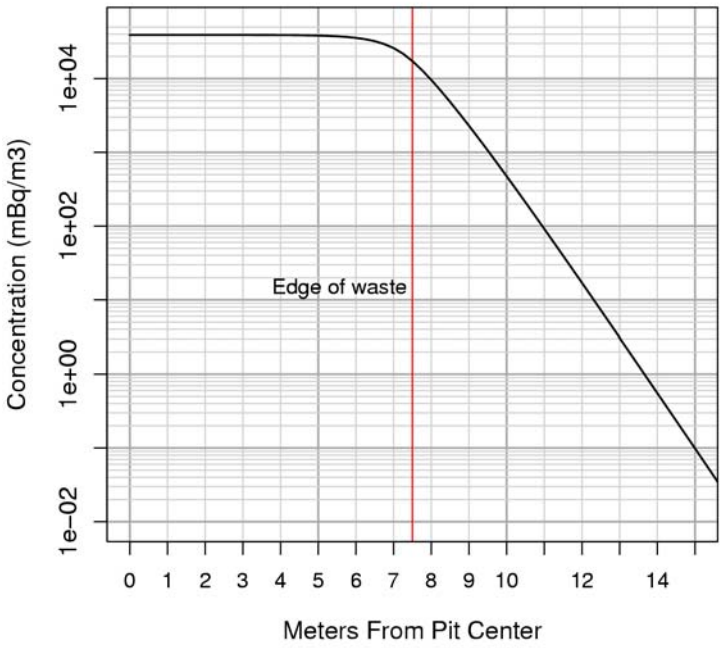

Figure 7.5. Concentration of Xe-133 (5-day) Along a Horizontal Line at Depth=0.75 meters Below Ground Surface

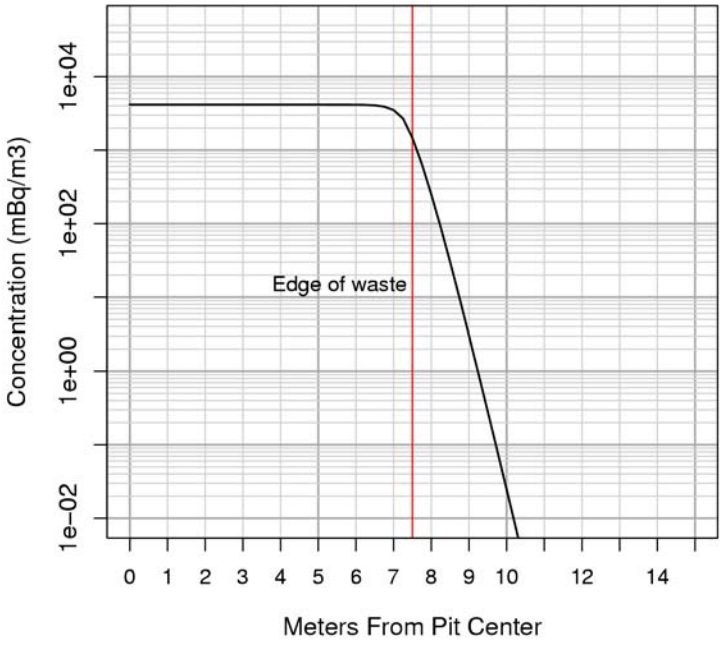

Figure 7.6. Concentration of Xe-135 (9-hr) Along a Horizontal Line at Depth=0.75 meters Below Ground Surface

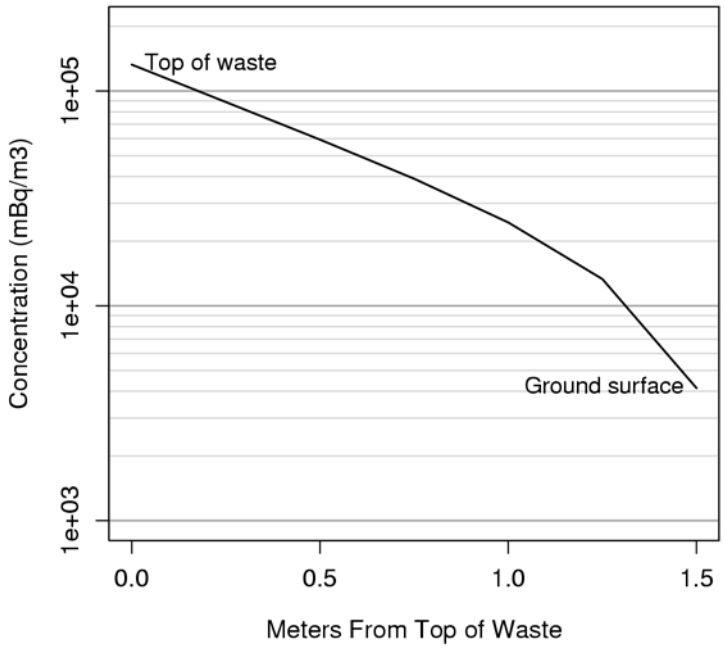

Figure 7.7. Concentration of Xe-133 (5-day) Along a Vertical Line at the Left Boundary

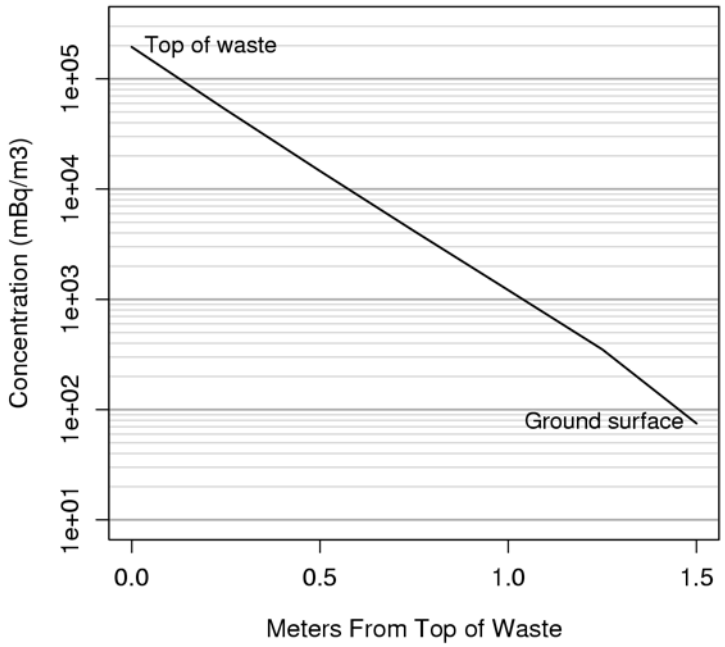

Figure 7.8. Concentration of Xe-135 (9-hr) Along a Vertical Line at the Left Boundary

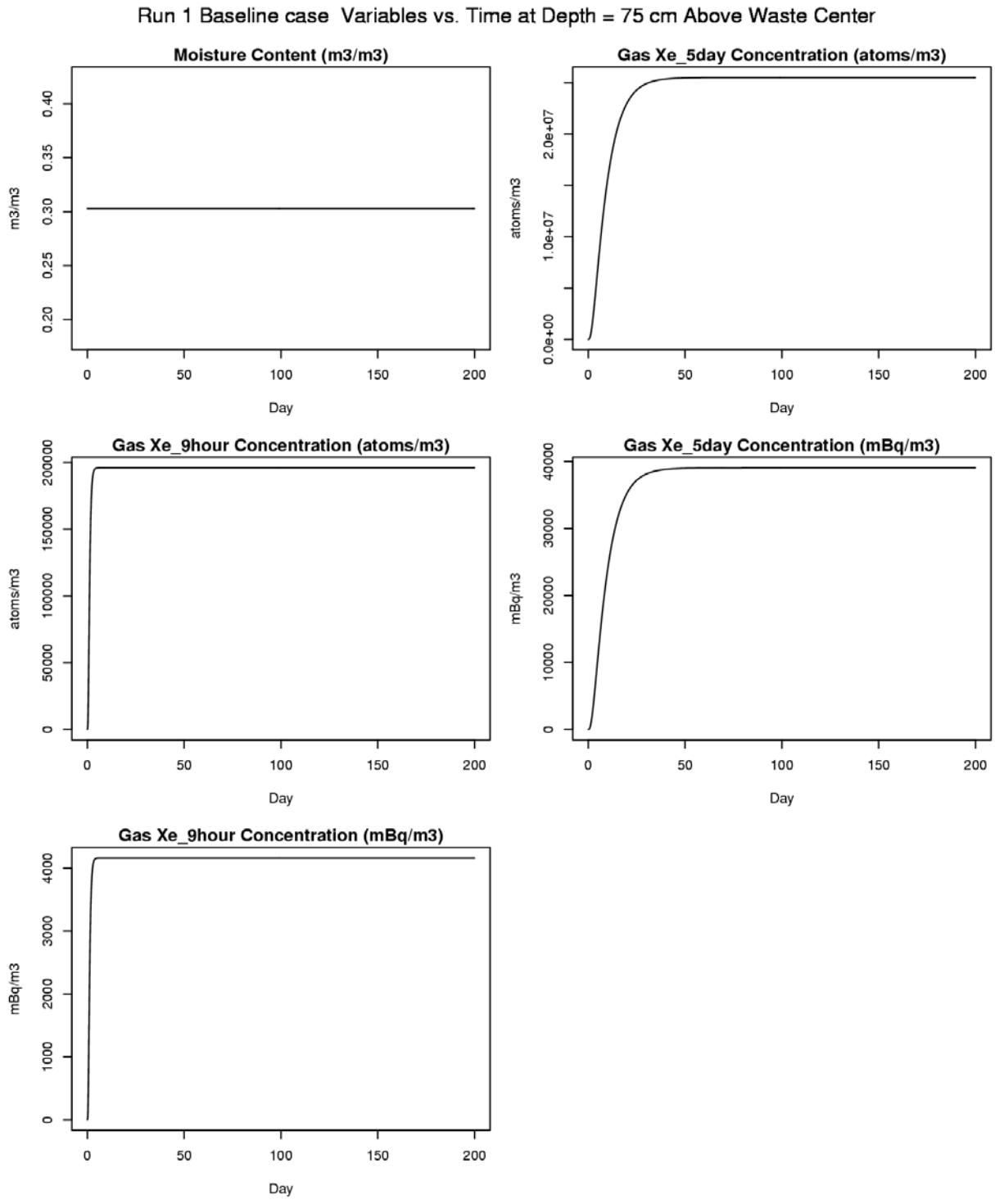

Figure 7.9. Simulated Variables vs. Time at 75 cm Below Ground Surface Along Waste Centerline

indicating nearly all of the xenon was in the gas phase. The predominance of gas-phase xenon was caused by the small water-gas partitioning coefficient (= 0.11) and low soil moisture content. The xenon-135 concentrations fall off more rapidly with distance from the waste form than do the xenon-133 concentrations, due to the shorter half life of xenon-135. However, the predicted concentrations at 75-centimeter depth are well above detection limits for the ARSA system (~0.58 mBq/m^3 for xenon-133 and 3 mBq/m^3 for xenon-135 - see Section 4.1). Points closer to the waste have still higher predicted concentrations.

The final results at the target node, 75 centimeters below ground surface along the waste centerline (left boundary of model domain), are shown in Table 7.4, along with the results of sensitivity analysis Cases 2 through 7, discussed in the following paragraphs.

Case 2. A test of linear scaling using a lower source release rate from Pit 12 yielded final concentrations that were in direct proportion to the lower release rate as compared to the Base case results from Pit 3, confirming scaling of xenon concentrations is linear.

Table 7.4. Results at End of Simulation for Node Located 75 cm Below Ground Surface at Waste Center

Case	Description	Moisture Content (m3/m3)	Concentrations (per m3 of air)			
			X-133 (atoms)	Xe-135 (atoms)	X-133 (mBq)	Xe-135 (mBq)
	Approximate Minimum Detection Limit (MDL):				**0.15**	**0.3**
	Results					
1	Baseline case	0.303	2.55E+07	1.96E+05	39,053	4,162
2	Test of linear scaling	0.303	3.06E+06	2.35E+04	4,690	498
3	Infiltration rate = 10 mm/yr	0.276	2.56E+07	2.97E+05	39,169	6,303
4	Residual saturation index in sediments = 0.20	0.277	2.54E+07	2.82E+05	38,922	5,996
5	Small tortuosity (factors: sediments = 1/3, basalt = 1)	0.303	3.23E+07	1.01E+06	49,376	21,496
6	Large tortuosity (factors: sediments = 1/5, basalt = 1/2)	0.303	3.27E+07	6.18E+05	50,031	13,128
7	Atmospheric pumping	0.303	2.49E+07	1.91E+05	38,023	4,048
	Percent change from base case					
1	Baseline case					
2	Test of linear scaling	0	-88.0	-88.0	-88.0	-88.0
3	Infiltration rate = 10 mm/yr	-8.9	0.3	51.5	0.3	51.5
4	Residual saturation index in sediments = 0.20	-8.5	-0.3	44.1	-0.3	44.1
5	Small tortuosity (factors: sediments = 1/3, basalt = 1)	-0.1	26.4	417	26.4	417
6	Large tortuosity (factors: sediments = 1/5, basalt = 1/2)	-0.1	28.1	215	28.1	215
7	Atmospheric pumping	0	-2.6	-2.7	-2.6	-2.7

Case 3. A lower infiltration rate of 10 mm/yr resulted in a slightly lower soil moisture than the base case, and no significant change in xenon-133 (5-day). However, the slight reduction in pore space saturation allowed a 50% increase in xenon-135 (9-hour) concentration, demonstrating greater sensitivity of the short-lived isotope to the amount of air-filled porosity.

Case 4. A lower (drier) residual saturation index for the Van Genuchten equation yielded results similar to those of Case 3.

Case 5. Constant tortuosity instead of the Millington and Quirk method was used. Tortuosities in this case were sediments = 3 and basalt = 1. These values are at the low end of a range suggested by INEEL. Tortuosity in both Case 5 and Case 6 was lower than the Millington and Quirk method, leading to faster diffusion of xenon and higher concentrations. The change in xenon-133 (5-day) was only about +25% compared to the base case, but the xenon-135 (9-hour) concentration quadrupled.

Case 6. Constant tortuosity at the upper end of the INEEL range. Tortuosities in this case were sediments = 5 and basalt = 2. The change in xenon-133 (5-day) was again about +25% compared to the base case, and the xenon-135 (9-hour) concentration was about twice the base case result.

Case 7 used a sinusoidal atmospheric pressure to introduce atmospheric pumping to the problem. Xenon concentrations were down slightly under this case.

Of all the results, the greatest sensitivity was found in the response of xenon-133 (5-day) to changing the tortuosity. The tortuosity had a much smaller effect on xenon-133. The lower tortuosities led to higher xenon concentrations. Linear scaling to lower source concentration in Case 2 had the next greatest impact, but modeled concentrations decreased by less than an order of magnitude.

8.0 Conclusions

Soil gas sampling for xenon isotopes is a technique that has promise for detection of TRU waste in the subsurface at RWMC. This technique is new but has shown success in proof-of-concept testing at the Hanford Site. Soil gas monitoring is a well established technique for locating organic contaminant sources in the subsurface. Noble gas analysis has also been successfully used to delineate tritium contamination through measurement of tritium's stable helium-3 decay product in soil gas. The technique builds on xenon isotope investigations performed in other disciplines so the analytical methodology is well established.

The proposed soil gas monitoring includes two related methods: monitoring of short lived radioxenon isotopes produced through spontaneous fission and monitoring of stable xenon also produced through spontaneous fission but possibly present from irradiated fuel materials. Monitoring of radioxenon isotopes will be successful only if the gas moves to the sampling point prior to decaying below detectable levels. Numerical modeling performed with the STOMP code indicates that radioxenon isotopes would remain many orders of magnitude above the detection limits given the average estimated plutonium-240 concentrations of the waste, assuming instantaneous release to the soil gas. Due to uncertainties in the nature and integrity of the waste forms, the degree of inhomogeneity of the waste, and the transport parameters, the method provides a semi-quantitative indication of the TRU concentration in the subsurface.

The greatest uncertainty in the model scenario is the amount of decay that occurs in the time it takes for the radioxenon gas to diffuse from the waste. That will depend on the waste form and the container integrity. The method of disposing of waste varied with time, as discussed in Section 2 with the waste stacked during some periods and not in others. In addition, efforts were made to compact some of the waste in situ. The compaction and more random disposal likely weakened container integrity and is expected to increase the release of xenon. Variation in the depth of the waste and cap thickness may also affect the results. Nonetheless, the principle is sound and there is room for considerable signal loss through decay while still detecting the radioxenon. The stable xenon isotopes are not subject to this decay-loss and should also be evaluated, although the atmospheric background means that it is a less sensitive technique. A stable xenon perturbation from fission products has been detected near a burial ground at the Hanford Site.

It would be beneficial to sample from several depths above and into the waste pits and at several distances from the waste unit during testing of the soil-gas sampling method at RWMC. This would provide site-specific information on the transport of the isotopes away from the waste and would aid in interpretation of results. Transects or grids across waste disposal sites then could be used to locate zones of suspect TRU.

9.0 References

Allègre CJ and SH Schneier. 1994. "The Evolution of the Earth." *Scientific American*, October 1994, pp. 66-75.

Bowyer TW, C Schlosser, KH Abel, M Auer, JC Hayes, TR Heimbigner, JI McIntyre, ME Panisko, PL Reeder, H Satorius, J Schulze, W Weiss. 2002. "Detection and Analysis of Xenon Isotopes for the Comprehensive Nuclear-Test-Ban Treaty International Monitoring System." *Jour. of Environmental Radioactivity*, V 59, pp. 139–151.

Bowyer TW, KH Abel, WK Hensley, CW Hubbard, AD McKinnon, ME Panisko, RW Perkins, PL Reeder, RC Thompson, and RA Warner. 1996. *Automatic Radioxenon Analyzer for CTBT Monitoring*. PNNL-11424, Pacific Northwest National Laboratory, Richland, Washington.

Dresel PE, KB Olsen, JI McIntyre, BM Kennedy, JC Hayes, DG Horton, AV Mitroshkov, and ME Panisko. 2003. "Xenon Isotopes in Soil Gas as Indicators of Buried Radioactive Waste [abstr]." *Geol. Soc. Am. Annual Meeting,* Seattle, Washington.

Ekström LP and RB Firestone. 2004. *WWW Table of Radioactive Isotope*s, database version 2/28/99 from URL http://ie.lbl.gov/toi/index.htm (version 2.1, Jan. 2004).

England TR and BF Rider. 1994. *ENDF-349. Evaluation and Compilation of Fission Product Yields 1993*. LA-UR-94-3106, Los Alamos National Laboratory, Los Alamos, New Mexico.

Fontaine J-P, F Pointurier, X Blanchard, T Taffary. 2004. *Atmospheric Xenon Radioactive Isotope Monitoring*. *Jour. of Environmental Radioactivity,* Vol. 72, pp. 129–135.

Freeze RA and JA Cherry. 1979. *Groundwater*. Prentice-Hall Inc., Englewood Cliffs, New Jersey.

Holden NE and DC Hoffman. 2000. "Spontaneous Fission Half-Lives for Ground-State Nuclides." *IUPAC Pure Appl. Chem*, Vol. 72, no. 8, pp. 1525-1562.

Holdren KJ, BH Becker, NL Hampton, LD Koeppen, SO Magnuson, TJ Meyer, GL Olson, and AJ Sondrup. 2002. *Ancillary Basis for Risk Analysis of the Subsurface Disposal Area*. INEEL/EXT-02-01125, Idaho National Environmental and Engineering Laboratory, Idaho Falls, Idaho.

Hudson GB. 1993. *Noble Gas Isotope Measurements for Spent Nuclear Fuel Reprocessing*. UCRL-ID-118658, Lawrence Livermore National Laboratory. Livermore, California.

Karoda PK and WA Myers. 2001. "Variation of the isotopic composition of xenon in the solar system." *Journal of Radioanalytical and Nuclear Chemistry*, Vol. 247, No. 2, pp. 248-283.

Kennedy BM, T Torgersen, and MC van Soest. 2002. "Multiple Atmospheric Noble Gas Components in Hydrocarbon Reservoirs: A Study of the Northwest Shelf, Delaware Basin, SE New Mexico. *Geochim et Cosmochem Acta,* Vol. 66, no. 16, pp. 2807-2822.

Klett A. 1999. "Plutonium Detection with a New Fission Neutron Survey Meter." *IEEE Trans. Nuc. Sci.*, Vol. 46, No. 4, pp. 877-879.

Magnuson SO and AJ Sondrup. 1998. *Development, Calibration and Predictive Results of a Simulator for Subsurface Pathway Fate and Transport of Aqueous and Gaseous Phase Contaminants in the Subsurface Disposal Area at the Idaho National Engineering and Environmental Laboratory*. INEL/EXT-97-00609, Lockheed-Martin Idaho Technologies Co., Idaho Falls.

McIntyre JI, KH Abel, TW Boyer, JC Hayes, TR Heimbigner, ME Panisko, PL Reeder, RC Thompson. 2001. "Measurements of ambient radioxenon levels using the automated radioxenon sampler/analyzer (ARSA)." *Journal of Radioanalytical and Nuclear Chemistry*, Vol. 248, No. 3, pp. 629–635.

McKinley KB and JD McKinney. 1978. *Initial Drum Retrieval Final Report.* TREE-1286, Idaho National Engineering and Environmental Laboratory, EG&G Idaho, Idaho Falls, Idaho.

Medici F. 2001. "The IMS Radionuclide Network of the CTBT." *Rad. Phys. and Chem,* Vol. 61, pp. 689-690.

Meshik AP, K Kehm, and CM Hohenberg. 2000. "Amonalous Xenon in Zone 13 Okelobondo. *Geochim. et Cosmochim. Acta,* Vol. 64, No. 9, pp. 1651-1661.

Millington RJ and JP Quirk. 1959. "Permeability of Porous Media." *Nature*, Vol. 183, pp. 387-388.

Olsen KB, PE Dresel, and JC Evans. 2001. *Measurement of Helium-3/Helium-4 Ratios in Soil Gas at the 618-11 Burial Ground*. PNNL-13675, Pacific Northwest National Laboratory, Richland, Washington.

Olsen KB, PE Dresel, GW Patton, JC Evans, and R Poreda. 2000. *Measurement of Tritium in Gas Phase Soil Moisture and Helium-3 in Soil Gas at the Hanford Townsite and 100 K Area*. PNNL-13217, Pacific Northwest National Laboratory, Richland, Washington.

Palcsu L, M Molnár, É Svingor, Zs Szántó, I Futó, T Pintér. 2001. "Dissolved Stable Noble as Measurements from Primary Water of Paks NPP [abstr]" from the Conference *Nuclear Energy in Central Europe 2001*, Institute of Nuclear Research of the Hungarian Academy of Sciences, Hungary.

Parrington JR, HD Knox, SL Breneman, EM Baum, and F Feiner. 1996. *Nuclides and Isotopes,* Fifteenth edition. General Electric Co. and KAPL, Inc., San Jose, California.

Poling BE, JM Prausnitz, and JP O'Connell. 2001. *The Properties of Gases and Liquids*, Fifth edition. McGraw-Hill, New York.

Pollack GL, RP Kennan, and JF Himm. 1989. "Solubility of Xenon in 45 Solvents including Cycloalkanes, Acids, and Alkanals: Experiment and Theory." *Jour. Chem. Phys.* 90 (11), pp. 6569-6575.

Porcelli D and GJ Wasserberg. 1995. "Mass Transfer of Helium, Neon, Argon, and Xenon through a Steady-State Upper Mantle. *Geochim. et Cosmochim. Act*a, Vol. 59, No. 23, pp. 4921-4937.

Schillebeeckx P, C Wagemans, AJ Deruytter, and R Barthélémy. 1992. "Comparative Study of the Fragments' Mass and Energy Characteristics in the Spontaneous Fission of ^{238}Pu, ^{240}Pu, and ^{242}Pu and in the Thermal-Neutron-Induced Fission of ^{239}Pu." *Nuclear Phys. A.* Vol. 545, pp. 623-645.

U.S. Department of Energy (DOE). 1996. *Plutonium: The First 50 Years*. DOE/DP-0137, U.S. Department of Energy, Washington, D.C.

Van Genuchten MTh. 1980. "A Closed Form Equation for Predicting the Hydraulic Conductivity of Unsaturated Soils." *Soil Soc. Sci. Am. J*. 44, pp. 892-898.

White MD and M Oostrom. 2000. *STOMP, Subsurface Transport Over Multiple Phases v. 2.0 Theory Guide*. PNNL-12030, Pacific Northwest National Laboratory, Richland, Washington.

White MD and M Oostrom. 2004. *STOMP, Subsurface Transport Over Multiple Phases v. 3.1 User's Guide*. PNNL-14478, Pacific Northwest National Laboratory, Richland, Washington.

www.ctbto.org. Preparatory Commission for the Comprehensive Test Ban Treaty.

Distribution

No. of Copies

OFFSITE

10 L. Hull
Idaho National Environmental and Engineering Laboratory
P.O. Box 1625, MS 2107
Idaho Falls, ID 83415-2107

No. of Copies

ONSITE

5 **Pacific Northwest National Laboratory**

P. E. Dresel (2)	K6-96
S. R. Waichler	K9-36
Hanford Technical Library (2)	P8-55